Journal of Chemical Science and Engineering
JCSE, 2(1): 45-52
www.scitcentral.com

Original Research Article: Open Access

# Green Synthesis of Reduced Graphene Oxide Nanosheets using Shikimic Acid for Supercapacitors

**Lien Thi Tran, Thanh Thuy Thi Tran, Hong Ngan Thi Le, Quang Minh Nguyen, Minh Dang Nguyen and Thu Ha Thi Vu***

*Key Laboratory for Petrochemical and Refinery Technologies, Ha Noi, Vietnam.*

*Received June 05, 2018; Accepted July 15, 2018; Published January 27, 2019*

## ABSTRACT

A new, green and efficient reducing agent (shikimic acid/SA) for graphene oxide reduction has been reported in this work. As a natural acid, shikimic acid is a green reductant so that reduction process is biocompatible and expedient for cost-effective mass production. Graphene oxide (GO) reduced by the shikimic acid has been studied by various physicochemical techniques. Electrochemical properties of rGO have been investigated by cyclic voltammetry and galvanostatic charge-discharge techniques. Results indicate that at a current density of 1 A $g^{-1}$ rGO exhibits a specific capacitance (SC) of 262 F $g^{-1}$ as a maximum value, and retains its capacity of about 90% after completing 1000 charge-discharge cycles. Therefore, rGO shows a great prospect of utilization as energy storage electrode material.

**Keywords:** Graphene, Shikimic acid, Supercapacitor, Reduced graphene oxide, Green chemistry

## INTRODUCTION

Nowadays, together with the social development, the demand for usage of energy has been always increasing, while sources of fossil fuels are quickly running out. As a result, finding or creating renewable energy sources, such as supercapacitors, batteries and fuel cells has been attracting a great amount of attention [1-4]. Out of those three, owning to their high rate of charge-discharge, large capacity and long-term cyclability [2,3,5], supercapacitors have been thoroughly investigated. Supercapacitors are split into two different branches, known as electrochemical double layer capacitors (EDLC) and pseudocapacitors, which are distinguished based on the energy storage principles. EDLC often use electrode materials with high surface area, for example activated carbon or its derivatives, and storage of electrical energy is received by separation of charge at the interface between an electrode and an electrolytic solution. Meanwhile, pseudocapacitors usually choose electrodes formed by metal oxides and charge is stored by chemical process related to reversible Faradaic charge-transfer.

In recent years, graphene has been viewed as electrocatalyst support because it holds several remarkably superior characteristics, for example high theoretical specific surface area, great thermal and electrical properties, and mechanical strength, and mass productibility [6-9]. With these listed advantages, graphene is one of the most chosen options as electrode material for EDLC. Among various methods to prepare graphene for EDLC [10-14], the chemical reduction of graphene oxide is the easiest and most popular to approach for its cost-effectiveness and potential for scale-up of production. The popularly employed reducing agents such as ethylene glycol [15], hydrazine hydrate [16] and hydrazine [17] are very toxic, harmful and/or explosive. Recent reports have focused on developing green and more eco-friendly reducing agents for replacement of hydrazine including sugar [18,19], ascorbic acid, vitamin C [20-22], humic acid [23]. In addition, caffeic acid, polyphenols of green tea [24,25] and even bacterial respiration [26,27] have also been used to fabricate reduced graphene oxides (rGO) as potential solutions to abovementioned problems.

Shikimic acid (3,4,5-trihydroxy-1-cyclohexene-1-carboxylic acid) is an organic compound existing naturally in assorted plants [28,29]. Derived from a cheap and largely available resource, anise (*Illicium verum*), shikimic acid can be easily extracted by different methods [29-31]. Not staying out of

**Corresponding author**: Thu Ha Thi Vu, Key Laboratory for Petrochemical and Refinery Technologies, No 2, Pham Ngu Lao Street, Hoan Kiem District, Ha Noi, Vietnam, Tel: +84 24 22189067; Fax: +84 24 39335410; E-mail: ptntd2004@yahoo.fr

**Citation:** Tran LT, Tran TTT, Le HNT, Nguyen QM, Nguyen MD, et al. (2019) Green Synthesis of Reduced Graphene Oxide Nanosheets using Shikimic Acid for Supercapacitors. J Chem Sci Eng, 2(1): 45-52.

the green chemistry trend, due to its non-toxicity and biocompatibility, shikimic acid is a necessary material in organic synthesis. Especially, in pharmaceutical industry, shikimic acid is known as an essential starting material for tamiflu production [32]. In order not to use toxic chemicals and carry out reactions at high temperature, this manuscript presents a simple, economical and environmental friendly route for the production of high quality rGO using shikimic acid as green reductant for supecapacitor. This technique is also appropriate for mass production because it is commercially available at an industrial level.

Physicochemical properties, structure and morphology of rGO nanosheets have been investigated by Ultra violet-visible (UV-Vis) spectra, X-ray diffraction (XRD), Raman, Fourier Transform InfraRed (FT-IR), X-ray photoelectron spectroscopy (XPS), thermogravimetric analysis (TGA), Atomic Force Microscopy (AFM) and transmission electron microscopy (TEM). The electrochemical behaviors were studied by cyclic voltametry and galvanostatic charge-discharge techniques to evaluate the expedience of rGO when used as supercapacitor electrode materials.

## EXPERIMENTAL

### Materials

All chemicals were of analytical grade and used as received. Expanded graphite was furnished by SGL Carbon GmbH (GFG). $H_2SO_4$ (96%), $KMnO_4$, $H_2O_2$ (30%), HCl (37%), ethanol and shikimic acid were all bought from Sigma Aldrich. All solutions were prepared by deionized water owning 18 MΩ $cm^{-1}$ in resistivity.

### Preparation of rGO

Firstly, graphene oxide (GO) was synthesized from graphite powder by the modified Hummers method as described by Tran et al. [33]. Dispersing the as-prepared GO was completely conducted with deionized water by ultrasonication for 3 h to reach a concentration of 0.1 mg $mL^{-1}$. Then, a mixture of diluted GO (100 mL) and shikimic acid at corresponding concentrations of 3 mM were sonicated for 30 min to obtain a homogeneous suspension solution. Next, it was heated to the suitable temperature, 60°C for 12 h and kept being uninterruptedly stirred with the purpose of avoiding aggregation during reaction process. Solid extracted from the fabricated product above after being centrifugated at 14500 rpm for 30 min was washed with water and ethanol. This process was repeated 3 times. The final product was dried at 45°C overnight in a vacuum oven.

### Characterization of GO and rGO

UV-Vis spectra were performed by Hach Dr400 UV-visible spectrophotometer. The particle size distribution of aqueous dispersion of GO and rGO was determined using Zetasizer Nano ZS (Malvern Instruments). Results of dynamic light scattering (DLS) analysis were collected after 3 times of measurements. X-ray diffraction (XRD) patterns of the as-prepared catalysts were recorded over the 2θ region of 5-70° using a D8 Advance diffractometer (Bruker) with CuKα radiation (λ=1.5405 Å). The diffractometer was operated at 40 kV, room temperature, at a scan rate of 0.05° $s^{-1}$. Raman spectroscopy was performed using a LabRam HR (Horiba Jobin Yvon) spectrometer with an argon ion laser (λ=514 nm) at ambient temperature. FT-IR spectra were recorded on a Nicolet 6700 Thermo Fisher. The morphology and microstructure of the catalysts were observed by a transmission electron microscope (TEM) JEOL JEM 2010 operated at 200 kV and Atomic Force Microscopy (AFM) multimode (Vecco) operated in the contact mode. Photoelectron spectra of selected catalysts were acquired with a Kratos AXIS ULTRA DLD spectrometer equipped with an Al kα monochromatic (hυ=1486.6 eV) X source. Thermogravimetric analysis (TGA) was performed under a nitrogen flow (10 mL min-1) on a Diamond TG/DTA analyzer (Perkin Elmer Instruments). Samples were heated from ambient temperature to 600°C at a heating speed of 10°C $min^{-1}$.

### Electrochemical experiments

Electrochemical experiments were conducted with a typical three-electrode cell at ambiant temperature on A PGS-ioc-HH12 Potentiostat/Galvanostat. The electrochemical measurements including cyclic voltammetry (CV) and galvanostatic charge-discharge were performed in 1 M $H_2SO_4$ aqueous electrolyte. A glassy carbon electrode (GCE) was chosen as working electrode; a saturated calomel electrode (SCE) was employed as the reference electrode; and a platinum wire was served as the counter electrode. All solutions were deaerated by pure nitrogen gas for 30 min prior to measurements. The equation (1) is to calculate the specific capacitance value (SC) of rGO, where I is discharging current (A); Δt indicates discharging time (s); m represents catalyst mass deposited on the GCE (g) and ΔV is discharging potential (V) for electrochemical testing.

$$SC\ (F\ g^{-1}) = \frac{I\ x\ \Delta t}{m\ x\ \Delta V} \qquad (1)$$

Based on the galvanostatic charge-discharge experiments, the Coulombic efficiency (η) can be calculated by the equation (2), in which $t_C$ and $t_D$ are the times of charging and discharging at the same current, respectively.

$$\eta = \left(\frac{t_D}{t_C}\right) x\ 100\% \qquad (2)$$

Results were collected after 3 times of measurements.

## RESULTS AND DISCUSSION

### Characterization of rGO

As shown in the inset in **Figure 1**, it is not difficult to distinguish GO and rGO based on their different colors, in which GO is in pale yellow while rGO is in black dispersion. The change in color during reaction implies that GO

transformed successfully into rGO in presence of shikimic acid as reducing agent. The reduction of GO is also examined by UV-Vis spectroscopy **(Figure 1)**. UV-Vis spectrum of GO illustrates an absorption peak appearing at 230 nm attributed to the $\pi \rightarrow \pi^*$ transition of the C–C bonds, and a peak ascribed to the $n \rightarrow \pi^*$ transition of the C=O bonds at 301 nm. After reduction, both of them vanished and gave way for an absorption band at 264 nm, meaning that GO was reduced and $sp^2$ carbon atoms in graphitic structure were restored [34]. Results of DLS analysis for GO and rGO seen from **Figure 1b** demonstrated the changes in the size of GO before and after reduction, where the average particle size (APS) of GO and rGO was 512 nm and 388 nm, respectively. Moreover, **Figure 1b** also indicated uniform size dispersion of these solutions, which is easily observed through average polydispersity index (PDI) of GO and rGO was 0.57 and 0.44, respectively. It might result from effect of ultrasonication when GO and rGO were redispersed.

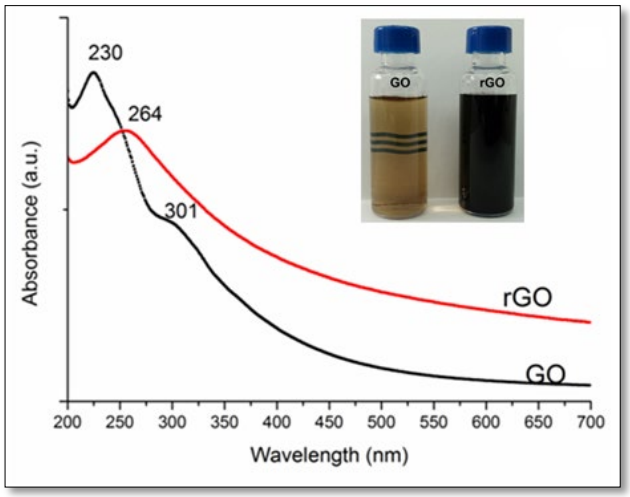


**Figure 1a.** UV-Vis spectra of GO and rGO. The inset shows the photographs for GO and rGO.

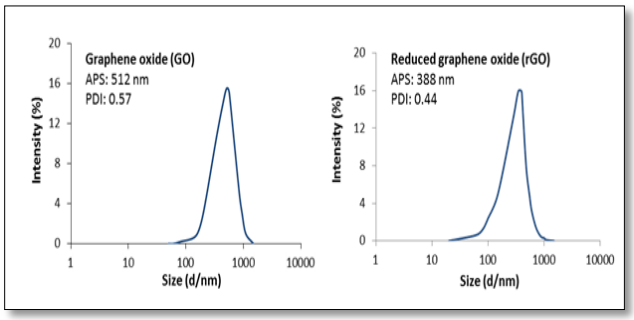


**Figure 1b.** Size distribution analysis on GO and rGO with respective PDI and size.

**Figure 2** illustrates XRD patterns of graphite, GO and rGO. The XRD pattern of graphite exhibits a strong peak at 2θ=26.6° corresponding to (002) reflection of the graphitic structure while XRD pattern of GO exhibits a peak located at ca. 11° assigned to the typical reflection peak of GO (002). After reduction, XRD pattern of rGO demonstrates the vanishing of the peak located at 11°, while a broad diffraction peak attributed to the (002) carbon peak of rGO appears between 2θ=24 and 26°, implying that GO was successfully reduced to rGO [35].

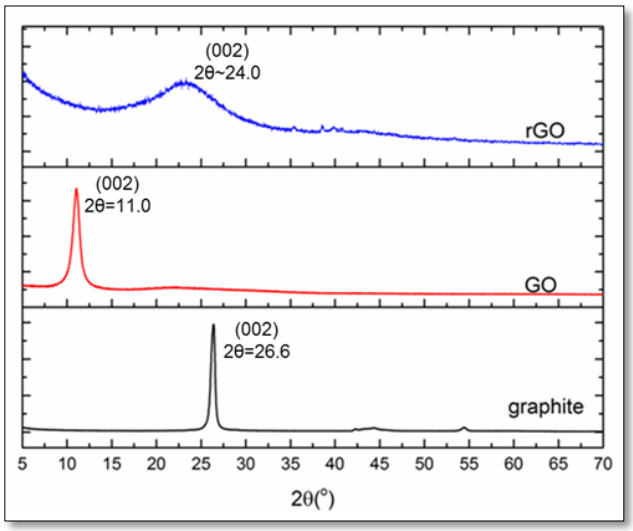


**Figure 2**. XRD spectra of graphite, GO and rGO.

The surface composition and the oxidation state of GO and rGO were determined by XPS results. As can be seen from **Figure 3a**, the C1s spectrum of GO can be deconvoluted in three components attributed to C-C (284.7 eV), C=O (286.6 eV) and C(O)OH (288.2 eV) bonds [36]. After reduction, there are almost no peaks to be recorded due to a striking decrease in intensities of C=O and C(O)OH. Meanwhile, a typical peak of C-C bond is seen with its significantly increasing intensity **(Figure 3b)**, which indicates successful deoxygenation of GO.

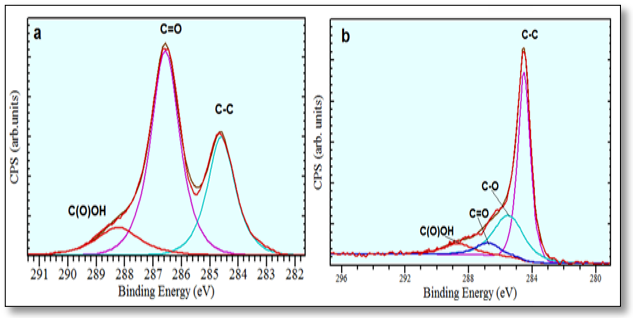


**Figure 3.** C1s XPS spectra of GO (a) and rGO (b).

The structural changes from GO to rGO after the reduction were also studied by Raman spectroscopy. It was observed from **Figure 4** that both GO and rGO showed signal of two characteristic peaks, where the peak of the G band at ca. 1594 $cm^{-1}$ was assigned to the in-plane bond-stretching vibration of $sp^2$ C-C bonds, while the D band at ca. 1349 $cm^{-1}$ identified the breathing modes of the graphitic domains, appearing in the existence of defected and disordered

graphite [37]. The ID/IG intensity ratios have been used to estimate defect level for graphene layers [38]. Indeed, after reduced by shikimic acid, ID/IG ratio of rGO (1.016) is greater than that of GO (0.896) indicating that there are more defects in the reduced graphene oxide structure, caused by reducing agents, thus reducing the size of the graphitic domains. This increase of ID/IG value matches with previous works of rGO synthesized by chemical reduction method [21,39]. The transformation from GO to rGO thanks to shikimic as reducing reagent was once again proved by Raman result.

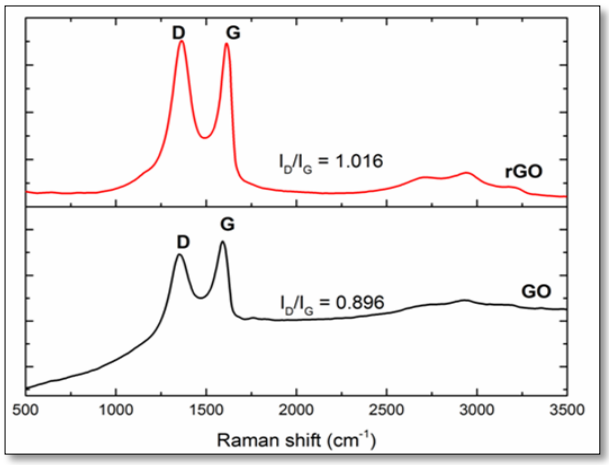


**Figure 4.** Raman spectra of GO and rGO.

The changes in the functional groups of GO before and after reduction were determined by FT-IR spectra **(Figure 5)**. For FT-IR spectra of GO, the peaks observed at 3450, 1727, 1640 $cm^{-1}$ resulted from stretching vibrations of O-H, C=O and aromatic C=C bonds, respectively. The two vibration bands appearing at ca. 1402, 1075 $cm^{-1}$ were ascribed to epoxy C-O bonds and alkoxy C-O bonds, respectively [40]. After reduction, the peak at 1727, 1402, 1075 $cm^{-1}$ can almost not be seen, additionally, intensity of the peak for O-H stretching bonds at 3450 $cm^{-1}$ significantly decreased, which confirmed removal of oxygen containing functional groups from GO.

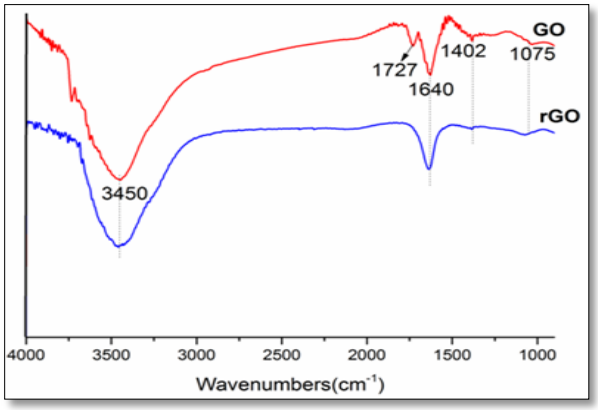


**Figure 5.** FT-IR spectra of GO and rGO.

According to **Figure 6**, thermogravimetric analysis in a $N_2$ atmosphere determined thermal stabilities of graphite, GO and rGO. No weight loss was observed in graphite conducted throughout the heating to 600°C. The total weight loss of GO in the same temperature condition was about 51.5%. In the region below 100°C, GO lost 17% of its weight due to evaporation of physisorbed water. On continuing to raise temperature to 250°C, GO showed a rapid 23.0% weight loss, resulting from the decomposition of labile oxygen containing functional groups [41]. For rGO, the total weight loss after the heating to 600°C was 29.3%, less than that of GO, which indicated that there was a significant decrease in the amount of functional groups on material surface after reduction or to put it in other way, GO was successfully reduced to rGO by shikimic.

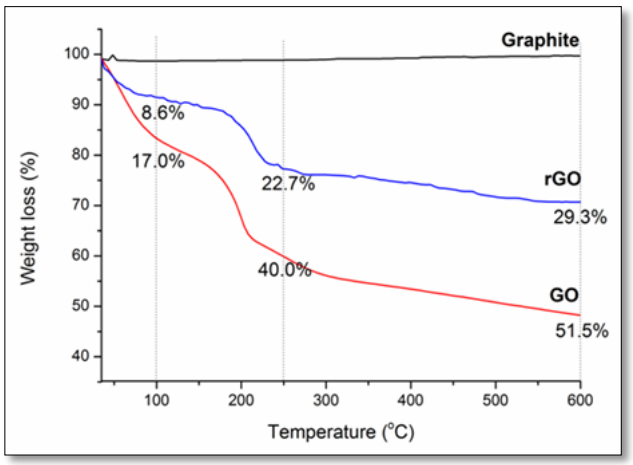


**Figure 6.** TGA plots of graphite, GO and rGO.

TEM images of GO and rGO are depicted in **Figure 7**. Obtained results shows that GO **(Figure 7a)** has the structure of micrometer-sized spread sheets with many wrinkles, while TEM images on **Figure 7b** exhibits that after reduction, graphene sheets kept its own super thin and almost transparent sheet structure, which is characteristic of few-layer structure of rGO.

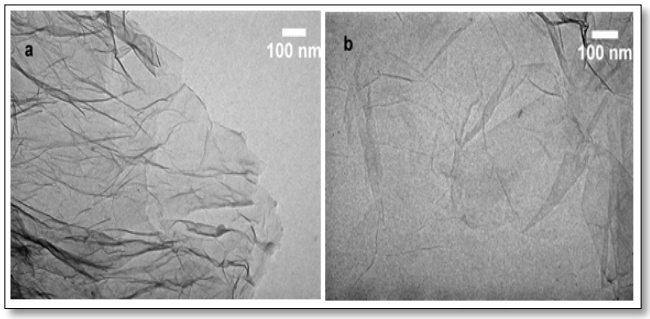


**Figure 7.** TEM images of GO (a), rGO (b).

### Electrochemical properties

Cyclic votammetry and galvanostatic charge-discharge were carried out with a three-electrode system from 0 to 1 V in 1 M $H_2SO_4$ solution to test the electrochemical performance of the as-obtained rGO. **Figure 8** showed that with the scanning rate increasing from 5 to 100 mV $s^{-1}$, all CV curves of rGO electrode exhibited the same shape, however, area covered by them increased, which proved its good capacitance behavior and rate capability. On the other hand, no redox peaks were observed throughout the scan region, signaling the typicality of the EDLC for carbon-based materials [1,14].

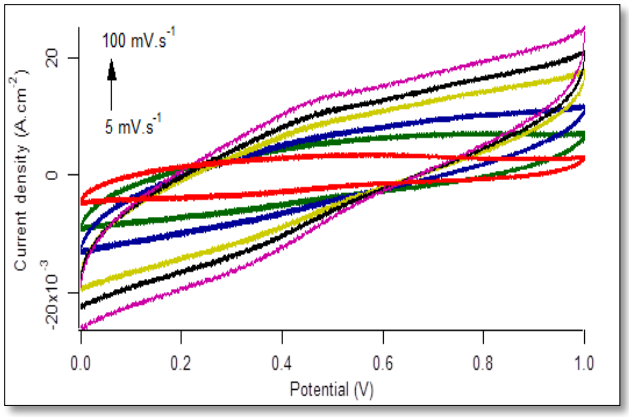


**Figure 8.** CV cuvres of rGO at different scan rates (three-electrode system).

**Figure 9** presents the charge-discharge curves of rGO electrode at various current densities from 1 to 5 A $g^{-1}$. These charge-discharge curves show triangular forms, which are symmetric and rather slope proving good capacitive quality of rGO electrode. Based on **Figure 9** and the abovementioned equation (1), at the current density of 1 A $g^{-1}$, the SC value of rGO electrode can be determined, 262 F $g^{-1}$.

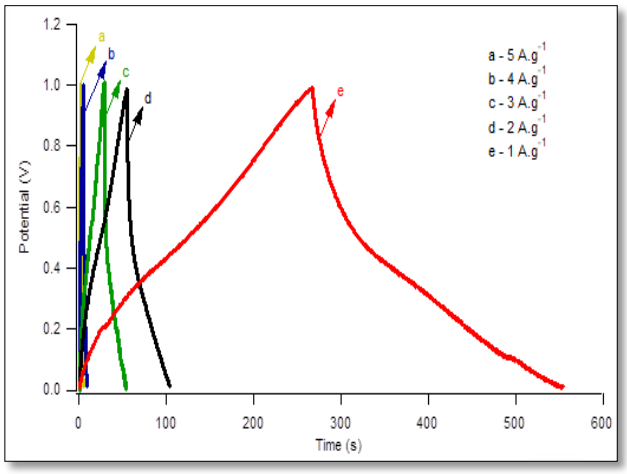


**Figure 9.** Galvanostatic charge-discharge curves of rGO at different current densities.

**Figure 10a** demonstrates its different charge-discharge cycles at the fixed current density of 1 A $g^{-1}$. Obtained graph illustrates series of isosceles triangle curves, which is reasonable with CV behavior of rGO and suggesting that its capacitance can maintain well. **Table 1** shows the comparison of SC of rGO electrode with reported values.

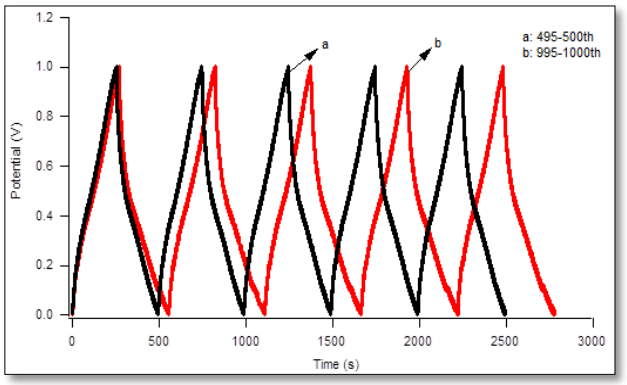


**Figure 10a.** The different cycles of rGO at 1 A $g^{-1}$.

**Table 1.** Comparison of electrochemical performances in terms of specific capacitance of various rGO electrodes.

| Sample | Electrode | Current density (A $g^{-1}$) | Specific capacitance (F $g^{-1}$) | Electrolyte | References |
|---|---|---|---|---|---|
| EdoX-GO | rGO | 1.0 | 255 | 6.0 M KOH | [42] |
| Graphene | Graphene nanosheets | 0.5 | 272 | 1.0 M $H_2SO_4$ | [23] |
| GMs | Graphene | 0.5 | 205 | 30% KOH | [43] |
| HRGO | rGO | 1.0 | 128 | 0.1 M $Na_2SO_4$ | [13] |
| rGO | rGO | 1.3 | 137 | 1.0 M $H_2SO_4$ | [39] |
| rGO | rGO | 1.0 | 262 | 1.0 M $H_2SO_4$ | This work |

In comparison with some previous works, it seems clear that rGO has a comparable SC value [23,42] and even much higher than that of HRGO - 128 F $g^{-1}$ [13], rGO - 137 F $g^{-1}$ [39] or rGO - 205 F $g^{-1}$ [43]. Another experiment to reassure about electrochemical stability of rGO electrode is cycling measurement. Still at the fixed current density of 1 A $g^{-1}$, **Figure 10b** displays the changes of Coulombic efficiency throughout 1000 continuous cycles in the potential range of 0 to 1 V. It is obvious that the SC of rGO electrode shows no significant change after 40 cycles, however, quickly increases to 242 F $g^{-1}$ up to 135 cycles. And then, it slightly increases and reaches the maximum value of 262 F $g^{-1}$ after 400 cycles. Based on the results from the galvanostatic charge-discharge graph, Coulombic efficiency could be calculated by applying equation (2). After 400 charge-discharge cycles are conducted, the SC initiates to slightly decrease and preserves at approximate 90% of the initial value, confirming good electrochemical cyclic stability in consecutive charge-discharge cycles.

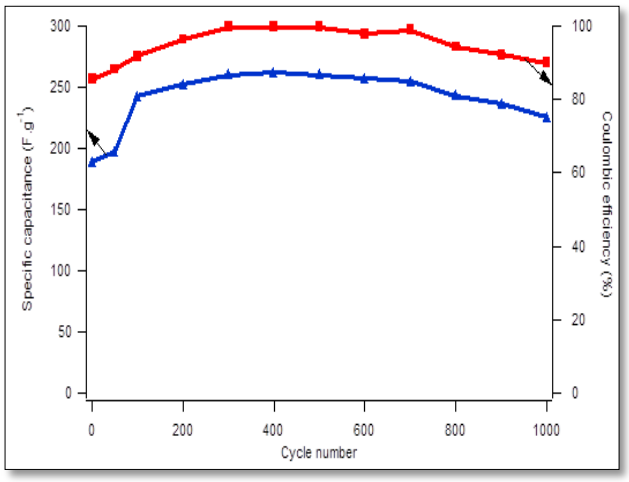


**Figure 10b.** Charge-discharge cyclic stability of rGO up to 1000 cycles, at a current density of 1 A $g^{-1}$.

## CONCLUSION

To sum up, we introduce the green, easy, and low-cost chemical way utilizing shikimic acid as reducing reagent to fabricate rGO nanosheets, opening up the possibilities in mass production of rGO. The as-prepared rGO was characterized by various physicochemical and electrochemical measurements. The obtained result demonstrates that in 1 M $H_2SO_4$ electrolyte solution, at the current density of 1 A $g^{-1}$, the as-synthesized graphene nanosheets exhibit high SC value (262 F $g^{-1}$). Besides, after completing 1000 charge-discharge cycles, the SC can retain nearly 90%, showing long-term cyclability. In addition, its high power density makes rGO an ideal electrode material for energy storage application.

## HIGHLIGHTS

- Graphene oxide was reduced by shikimic acid, an eco-friendly reagent.
- The reduction of the graphene oxide nanosheets was confirmed by various characterization methods.
- The obtained reduced graphene oxide is few layer nanosheets.
- The as-synthesized rGO exhibits high SC value and long-term cyclability.

## ACKNOWLEDGEMENT

The authors gratefully acknowledge the financial supports from the Project Management Unit of FIRST, for this sub-project through grant agreement No.06/FIRST/2a/KEYLABPRT and Ministry of Industry and Trade (Vietnam) through contract No. 077.17.ĐT/HĐ-KHCN.

## REFERENCES

1. Yang W, Gao Z, Wang J, Wang B, Liu Q, et al. (2012) Synthesis of reduced graphene nanosheet/urchin-like manganese dioxide composite and high performance as supercapacitor electrode. Electrochimica Acta 69: 112-119.
2. Simon P, Gogotsi Y (2008) Materials for electrochemical capacitors. Nat Mater 7: 845-854.
3. Zhang LL, Zhao XS (2009) Carbon-based materials as supercapacitor electrodes. Chem Soc Rev 38: 2520-2531.
4. Liu C, Li F, Ma LP, Cheng HM (2010) Advanced materials for energy storage. Adv Mater 2: E28-E62.
5. Nyholm L, Nystrom G, Mihranyan A, Maria Strømme (2011) Towards flexible polymer and paper-based energy storage devices. Adv Mater 23: 3751-3769.
6. Novoselov KS, Geim AK, Morozov SV, Jiang D, Zhang Y, et al. (2004) Electric field effect in atomically thin carbon films. Science 306: 666-669.
7. Geim AK, Novoselov KS (2007) The rise of graphene. Nat Mater 6: 183-191.
8. Li D, Mueller MB, Gilje S, Kaner RB, Wallace GG (2008) Processable aqueous dispersions of graphene nanosheets. Nat Nanotechnol 3: 101-105.
9. Stankovich S, Dikin DA, Dommett GHB, Kohlhaas KM, Zimney EJ, et al. (2006) Graphene-based composite materials. Nature 442: 282-286.
10. Ke Q, Wang J (2016) Graphene-based materials for supercapacitor electrodes - A review. J Materiomics 2: 37-54.

11. Marcelina V, Syakir N, Wyantuti S, et al. (2017) Characteristic of thermally reduced graphene oxide as supercapacitors electrode materials. IOP Conference Series: Material Science and Engineering 196: 012034.

12. Martinez JG, Otero TF, Bosch-Navarro C, Coronado E, Mart-Gastaldo C, et al. (2012) Graphene electrochemical responses sense surroundings. Electrochimica Acta 81: 49-57.

13. Wang C, Zhou J, Du F (2016) Synthesis of highly reduced graphene oxide for supercapacitor. J Nanomater 2016: 1-7.

14. Karthika P, Rajalakshmi N, Dhathathreyan K (2012) Functionalized exfoliated graphene oxide as supercapacitor electrodes. Soft Nanosci Lett 2: 59-66.

15. Liu Y, Zhang Y, Ma G, Wang Z, Liu K, et al. (2013) Ethylene glycol reduced graphene oxide/polypyrrole composite for supercapacitor. Electrochimica Acta 88: 519-525.

16. Zhu P, Shen M, Xiao S, Zhang D (2011) Experimental study on the reducibility of graphene oxide by hydrazine hydrate. Physica B 406: 498-502.

17. Park S, An J, Potts JR (2011) Hydrazine-reduction of graphite- and graphene oxide. Carbon 49: 3019-3023.

18. Zhu C, Guo S, Fang Y, Dong S (2010) Reducing sugar: New functional molecules for the green synthesis of graphene nanosheets. ACS Nano 4: 2429-2437.

19. Akhavan O, Ghaderi E, Aghayee S, Fereydoonia Y, Talebi A (2012) The use of a glucose-reduced graphene oxide suspension for photothermal cancer therapy. J Mater Chem 27: 13773-13781.

20. Zhang J, Yang H, Shen G, Cheng P, Zhang J, et al. (2010) Reduction of graphene oxide via L-ascorbic acid. Chem Commun 46: 1112-1114.

21. Fernández-Merino MJ, Guardia L, Paredes JI, Villar-Rodil S, Fernandez PS, et al. (2010) Vitamin C is an ideal substitute for hydrazine in the reduction of graphene oxide suspensions. J Phys Chem C 114: 6426-6432.

22. Gao J, Liu F, Liu Y, Ma N, Wang Z, et al. (2010) Environment-friendly method to produce graphene that employs vitamin C and amino acid. Chem Mater 22: 2213-2218.

23. Xing B, Yuan R, Zhang C, Huang G, Guo H, et al. (2017) Facile synthesis of graphene nanosheets from humic acid for supercapacitors. Fuel Process Technol 65: 112-122.

24. Vu THT, Tran TTT, Le HNT, Nguyen PHT, Bui NQ, et al. (2015) A new green approach for the reduction of graphene oxide nanosheets using caffeine. Bull Mater Sci 38: 667-671.

25. Akhavan O, Kalaee M, Alavi ZS, Esfandiar A, Ghiasi SMA (2012) Increasing the antioxidant activity of green tea polyphenols in the presence of iron for the reduction of graphene oxide. Carbon 50: 3015-3025.

26. Akhavan O, Ghaderi E (2010) Escherichia coli bacteria reduce gaphene oxide to bactericidal graphene in a self-limiting manner. Carbon 50: 1853-1860.

27. Salas EC, Sun Z, Luttge A, Tour JM (2010) Reduction of graphene oxide via bacterial respiration. ACS Nano 4: 852-4856.

28. Cardoso SF, Lopes LMX, Nascimento IR (2014) Eichhornia crassipes: An advantageous source of shikimic acid. Rev Bras Farmacogn 24: 439-442.

29. Ghosh S, Chisti Y, Banerjee UC (2012) Production of shikimic acid. Biotechnol Adv 30: 1425-1431.

30. Enrich LB, Scheuermann ML, Mohadjer A, Matthias KR, Eller CF, et al. (2008) *Liquidambar styraciflua*: A renewable source of shikimic acid. Tetrahedron Lett 49: 2503-2505.

31. Cai M, Luo Y, Chen J, Liang H, Sun P, et al. (2014) Optimization and comparison of ultrasound-assisted extraction and microwave-assisted extraction of shikimic acid from Chinese star anise. Sep Purif Technol 133: 375-379.

32. Rawat G, Tripathi P, Saxena RK (2013) Expanding horizons of shikimic acid. Recent progresses in production and its endless frontiers in application and market trends. Appl Microbiol Biotechnol 97:4277-4287.

33. Tran DNH, Kabiri S, Losic D (2014) A green approach for the reduction of graphene oxide nanosheets using non-aromatic amino acids. Carbon 76: 193-202.

34. Ang PK, Wang S, Bao Q, Thong JT, Loh KP (2009) High-throughput synthesis of graphene by intercalation-exfoliation of graphite oxide and study of ionic screening in graphene transistor. ACS Nano 3: 3587-3594.

35. Qiu JD, Wang GC, Liang RP, Xia XH, Yu HW, et al. (2011) Controllable deposition of platinum nanoparticles on graphene as an electrocatalyst for direct methanol fuel cells. J Phys Chem 115: 15639-15645.

36. Stankovich S, Dikin DA, Piner RD, Kolhaas KA, Kleinhammes A, et al. (2007) Synthesis of graphene-based nanosheets via chemical reduction of exfoliated graphite oxide. Carbon 45: 1558-1565.

37. Tuinstra F, Koenig J (1970) Raman spectrum of graphite. J Phys Chem 53: 1126.

38. Kudin KN, Ozbas B, Schniepp HC, Prud'homme RK, Aksay IA, et al. (2007) Raman spectra of graphite oxide and functionalized graphene sheets. Nano Lett 8: 36-41.

39. Jana M, Saha S, Khanra P, Murmu NC, Srivastava SK, et al. (2014) Bio-reduction of graphene oxide using drained water from soaked mung beans (*Phaseolus aureus* L.) and its application as energy storage electrode material. Mater Sci Eng 186: 33-40.

40. Garrigues JM, Bouhsain Z, Garrigues S, de la Guardia M (2000) Fourier transform infrared determination of caffeine in roasted coffee samples. Fresenius J Anal Chem 366: 319-322.

41. Kuila T, Bose S, Khanra P, Mishra AK, Kim NH, et al. (2012) A green approach for the reduction of graphene oxide by wild carrot root. Carbon 50: 914-921.

42. Abdelkader AM (2015) Electrochemical synthesis of highly corrugated graphene sheets for high performance supercapacitors. J Mater Chem 3: 8519-8525.

43. Wang Y, Shi Z, Huang Y, Ma Y, Wang C, et al. (2009) Supercapacitor devices based on graphene materials. J Phys Chem C 113: 13103-13107.